CURRENT FLUCTUATIONS OF REVERSE-BIASED SOLAR CELLS

Ľubomír Škvarenina
Doctoral Degree Programme (1), FEEC BUT
E-mail: xskvar01@stud.feec.vutbr.cz

Supervised by: Robert Macků
E-mail: macku@feec.vutbr.cz

Abstract: This paper presents mainly noise diagnostics of *pn* junctions local defects in a single-crystalline silicon solar cells structure. Research consists of a non-destructive measurement methodology of reverse-biased junction in solar cells. Diagnostics of defect areas in this documents are based especially on measurement of noise power spectral density, measurement of the radiation emitted from defects in visible range and *I*-*V* characteristic measurement.

Keywords: Solar Cells, Silicon, Noise Spectroscopy, Diagnostics, Defects, Flicker Noise

1 INTRODUCTION

This document deals with noise diagnostic of *pn* junction in semiconductor devices. Solar cell operation is based on the generation of electron-hole pairs in the transition region, and the separation of both types of carriers by the junction electric field [1]. Measurements of reverse-biased *pn* junctions can provide valuable information of the solar cells and their defects. We will present mainly the measurement of the current noise power spectral density of the solar cell for various reverse voltages. Diagnostics of defect areas can be carried out by one or several of the following methods: scanning the time response of the reverse current, measurement of *I*-*V* characteristics, measurement of RMS value of narrowband current noise for reverse current or voltage, measurement of noise power spectral density, measurement of the radiation emitted from the defect during microplasma discharge formation (see [2]). The latter method is applicable to optoelectronic devices [3].

The nature of the observed noise depends on the voltage (current) bias applied to solar cells. This can be attributed to variations in the electric stress and/or origin of breakdowns. Thanks to this fact, our study is strictly divided into reverse and forward-bias conditions. With regard to the paper scope, only reverse-biased specimens will be studied here [4].

2 EXPERIMENTAL SET-UP

The complete schematic diagram for a noise measurement system of the solar cells is shown on fig. 1. The most important part of the measurement system is a metal box (serves as a shielding) with a solar cell fragment. The sample is placed in the box between two conductive aluminium electrodes with a paper around to avoid precaution against short circuit and leakage effects. A capacitor ($C = 2.2\,\mu\text{F}$), which is used for stabilization of the current from a low noise voltage source Agilent E3631A (a linear source with maximum output power of 80 W), is on the input of the circuit. An electrically isolated output in positive range of $0 \div 25\,\text{V}/1\,\text{A}$ was used on this triple-output power supply. Double-shielded coaxial cables terminated with BNC connectors (marked with brown color on fig. 1) are strictly used in the circuit. That are a low noise versions containing a semiconducting layer of graphite[1] between the core and the screen. As stated before, the solar cell is reverse-biased

[1] This conducting layer does not change the dielectric properties of the cable.

between conductive electrodes. The circuit is closed by resistor ($R = 5.517\,\Omega$) where the noise signal is detected. The resistance of resistor is much smaller than the sample operation point resistance and resistance of permanently ionized defects channels, however, large enough to provide sensing authentic noise signal. Subsequently, the noise signal is amplified by a ultra low-noise preamplifier Signal Recovery 5184 with a pseudo-differential input and a single-ended output via BNC connectors. It has a frequency response of $0.5\,\mathrm{Hz} \div 1\,\mathrm{MHz}$ and a fixed voltage gain of $\times 1000$ (60 dB). The input impedance of the voltage preamplifier is of $5\,\mathrm{M\Omega}$ (50 pF). The noise background of preamplifier is about of $800\,\mathrm{pV \cdot Hz^{-1/2}}$ at 1 kHz. The signal applied to the baseband input Rohde & Schwarz FMU36 Baseband Analyzer is on the single-ended output of the amplifier. It is a FFT-based spectrum analyzer with the frequency range of $10\,\mathrm{Hz} \div 36\,\mathrm{MHz}$ and the selectable input impedance of $50\,\Omega / 1\,\mathrm{M\Omega}$. The signal was connected to the Q baseband input of the analyzer. The advantage of this analyzer is high sensitivity also at low frequencies to analyze extremely weak signals. Despite that fact, it was necessary to use an preamplifier for relatively poor noise background of the analyzer.

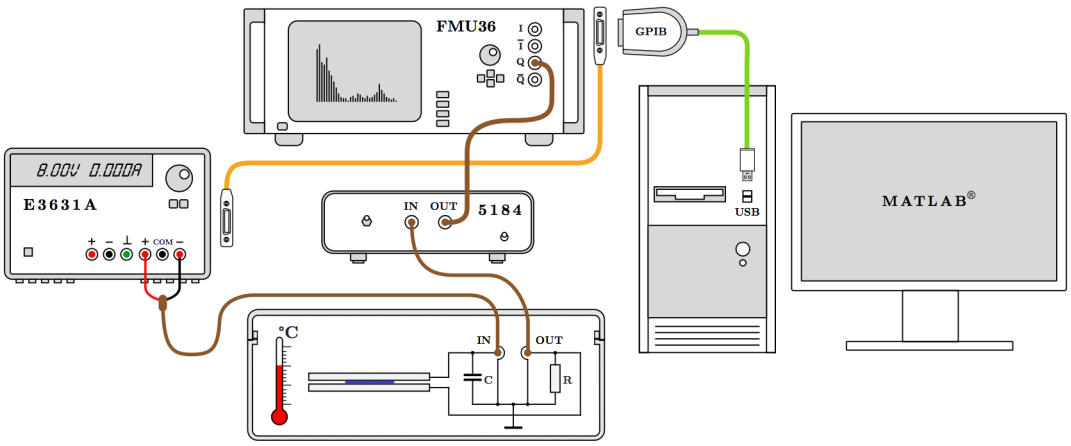

Figure 1: Experimental set-up of measurement system.

Power supply E3631A is interconnected with the baseband analyzer FMU36 via 8-bit parallel multi-master interface bus standard IEEE-488.2 commonly called GPIB (General Purpose Interface Bus). Both instruments are finally connected through Agilent 82357B USB/GPIB interface with PC using MATLAB®. The instrumentation system comprising hardware bus GPIB required software standard VISA (Virtual Instrument Software Architecture) implemented in Instrument Control Toolbox™ for configuration. Instruments are controlled by sending and receiving text-based (ASCII) commands under standard SCPI (Standard Commands for Programmable Instruments).

The voltage-bias from 8 V to 15 V in increments of 1 V was set on the power supply. The noise is neglectable small bellow this interval and strong electric field can cause damage of sample above this interval. The input impedance of the baseband analyzer was setted to $1\,\mathrm{M\Omega}$. The FFT-based spectrum measurement for one voltage-bias was carried out in range of 10 Hz to 1 MHz with 120 points. The center frequency for each point was selected in logarithmic scale. The frequency span (frequency display range) was set to 10% of the central frequency and it was subsequently dynamically changed depending on it. However, this set-up is applied for frequencies higher than 100 Hz because the specification of analyzer allowed to set a minimum span to 10 Hz for working in the frequency domain (option 0 Hz automatically switch to the time domain). For this reason the span was fixed on 10 Hz for frequencies lower than 100 Hz. The trace measurement in single sweep mode for each bandwidth

consists of 16 sweeps with 625 measurement points acquired during a sweep. The one trace of consecutive sweeps was stabilized by averaging to suppress noise spikes. Each trace for the specific center frequency was used for median calculation and one power spectral density point was obtained (see fig. 3).

The radiation generated from reverse-biased *pn* junction defects is used to study the near-field or far-field local properties. It proves to be useful to measure surface radiation and to make light spots localization. It is also used to measure the radiation intensity versus voltage plot, its correlation with other, mainly noise characteristics and the radiation spectrum [4]. A scientific CCD camera type G2-3200 was used for measure the radiation from a solar cell *pn* junction in optical far-field configuration. The camera is equipped with a silicon chip CCD Kodak KAF-3200ME[2]. The electronics of the camera use 16-bit ADC with double correlated sampling which ensures high dynamic range. The silicon chip has 3.2 MPx (2184×1472) resolution and it is cooled by dual system of Peltier's modules with the typical operation temperature $T = 45\,°\mathrm{C}$ under the ambient temperature to minimize dark current. The dark current of an optical sensor for a single pixel ($6.8\,\mu\mathrm{m} \times 6.8\,\mu\mathrm{m}$) is $0.8\,\mathrm{e}\cdot\mathrm{s}^{-1}$ at $T = 0\,°\mathrm{C}$. A lens with focal ratio 1.2 and working aperture 41.7 mm was used with the camera. The measurement was carried out for a range of wavelengths from 300 nm to 1050 nm with a exposure time of 300 s. The CCD chip mean quantum efficiency <QE> = 0.514 is reached in the interval from 300 nm to 1050 nm. The sample reverse-bias voltage 9 V is realized by the constant-current source Keithley 6220 DC (see fig. 4).

3 RESULTS AND DISCUSSION

Our experiments carry out that spectrum noise varies and it is nonstacionary for relatively long initiation time. Any other process or other type of noise was not detected for sample N1. The *I-V* characteristic is smooth function as can be seen on fig. 2. Any breakdowns are not apparent in a solar cell structure. The specimen under investigation did not show observable breakdowns or other predominant effects, capable of affecting the measurement results undesirably [6].

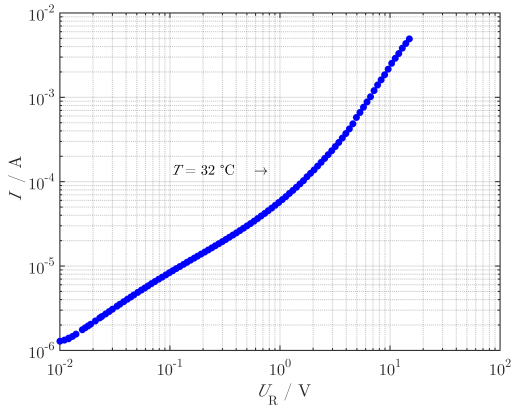

Figure 2: Current-voltage characteristic of reverse-biased solar cell, sample N1.

Nevertheless, local defects exist and it was demonstrated by optical measurement (see fig. 4). Defects integrally increase reverse current and *I-V* curve seems to be partially linear (resistive-like) and it does not show any anomaly.

The measurement of voltage noise power spectral density for all mentioned voltage levels takes about 12 hours (1.5 hours for each one). The behaviour of power spectral density is showed on fig. 3

[2]For spectral response and quantum efficiency see [5]

for various reverse-bias voltages applied to the specimen under investigation. It is clear that the measurement in fig. 3 corresponds to the only one type of noise. The noise power is approximately inversely proportional to the frequency at whole spectrum. In addition, apparent noise floor exhibits voltage dependence. Fig. 3 indicates only the presence of f^{-1} noise (known as flicker noise) for all

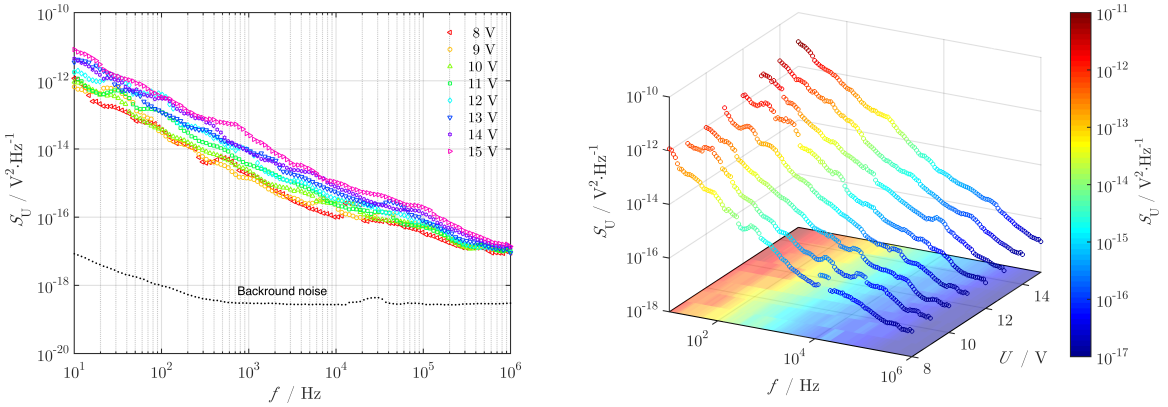

(a) (b)

Figure 3: Noise power spectral density of reverse-biased solar cell for various reverse voltages, sample N1.

reverse-bias voltages, however, fundamentally background of these processes is not known yet [6]. It has been shown during many years of noise research that f^{-1} noise is closely related to the specimen bulk homogeneity being impaired, for example, by the presence of impurities or defects in the crystal lattice [7].

The radiation intensity of a solar cell measured with camera is converted to photons per second (photon flux Φ_q). As can be seen on fig. 4 the current does not flow by edges but it is flowing through local areas (light spots). That light spots areas are naturally stressed and our assumption is that these exposed areas produce electrical noise. In view of the fact that these areas are substantially stressed,

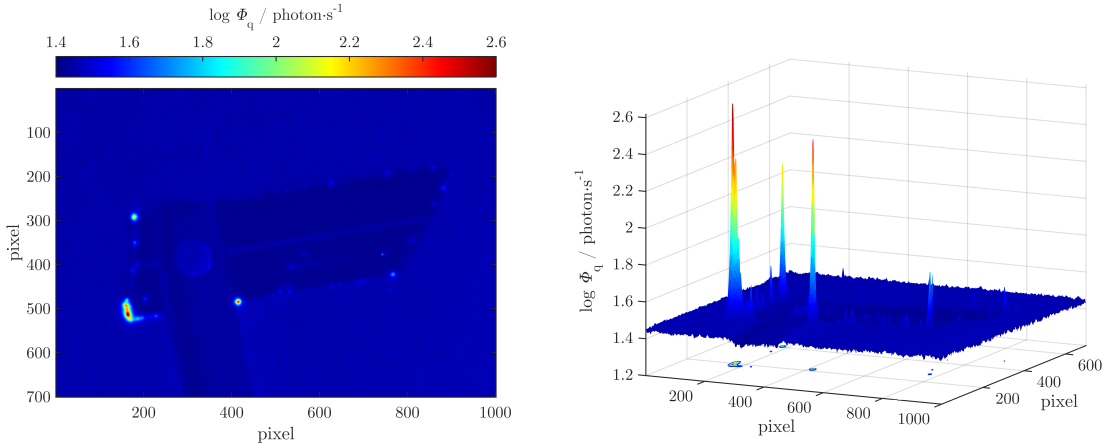

(a) (b)

Figure 4: Photography of measured solar cell with light defect spots, sample N1, bias reverse voltage $U_R = 9\,\mathrm{V}$, temperature $T = 26\,^{\circ}\mathrm{C}$, area $30.68\,\mathrm{mm}^2$, perimeter $26.95\,\mathrm{mm}$.

increase its cross-section, ordinary operation can cause complete degradation of the material. The number of the defect areas perhaps increase gradually. It is definitely very interesting on fig. 4(b) that

the solar cell generated radiation is lower than its surrounding neighborhood. This indicates the basic premise that the solar cell absorbs the light.

4 CONLUSION

Dependence of the power noise spectral voltage density $S_U(f)$ was investigated in the frequency range of 10 Hz to 1 MHz for a single-crystal solar cell in this paper. The noise spectra magnitude increase with increasing reverse voltage from 8 V to 15 V monotonically. The voltage noise power spectral density was only in a form of f^{-1} noise in this investigation. Future research will be based on a defective area modification by focusing ion machining (vaporizing the material) and then monitor deviations on noise measurements which are very sensitive. Subsequently we will try to explain the nature of the defect depending on the noise deviations.

ACKNOWLEDGEMENT

This work was supported by the European Union within the framework of the project CZ.1.07/2.3.00/-30.0039 "Excellent young researchers at Brno University of Technology", by the SIX research centre CZ.1.05/2.1.00/03.0072 and Centre of Excellence CEITEC CZ.1.05/1.1.00/02.0068.

REFERENCES

[1] J.P. COLINGE and C.A. COLINGE. *Physics of Semiconductor Devices*. Springer, 2002.

[2] P. KOKTAVÝ and R. MACKŮ. Noise and optical activities of local defects in solar cells pn junctions. In *ICNF2011: 2011 21st International Conference on Noise and Fluctuations*, pages 409–412, Kanada, Toronto, 2011. IEEE. ISBN: 978-1-4577-0191- 7.

[3] R. MACKŮ and P. KOKTAVÝ. Impact of local defects on photon emission, electric current fluctuation and reliability of silicon solar cells studied by electro-optical methods. *ElectroScope*, pages 38–43, 2011. ISSN: 1802-4564.

[4] R. MACKŮ, J. ŠICNER, and D. DALLAEVA. An experimentally based characterization of solar cell structure defects by means of noise and optical activities analysis. *Fracture Mechanics for Durability, Reliability and Safety*, pages 499–506, August 2012. ISBN: 978-5-905576-18- 8.

[5] Eastman Kodak Company. *KAF-3200ME Performance Specification*, 2 edition, May 2002. Available on September 2015 from <http://www.yankeerobotics.com/trifid/dnload/KAF-3200ME.pdf>.

[6] R. MACKU and P. KOKTAVÝ. Improved electrical characterization of silicon solar cells based on noise spectroscopy in forward direction. In *Proceedings of 24rd European Photovoltaic Solar Energy Conference*, pages 484–488. WIP-Renewable Energies, 2009. ISBN: 3-936338-24- 8.

[7] L. K. J VANDAME. Noise as a diagnostic tool for quality and reliability of electronic devices. *IEEE Transaction on electron device*, vol. 41 (No. 11), November 1994.